2ème conférence Internationale des énergies renouvelables CIER-2014
Proceedings of Engineering and Technology - PET

Buoyancy induced flow in a nanofluid filled enclosurepartially exposed to forced convection

A. Dayf[a], M. Feddaoui[a,§], A. Azzabakh[a], H. Meftah[a], N. Labsi[b]

[a]*Laboratoire Génie Energie, Matériaux et Systèmes (LGEMS)*
Ecole Nationale des Sciences Appliquées ENSA, B.P. 1136, Agadir – Morocco
[b]*Laboratoire des Phénomènes de Transfert*
Université des Sciences et de la Technologie Houari Boumediene USTHB,
B.P. 32, El-Alia Bab-Ezzouar, 16111 Algiers, Algeria.
[*]*Corresponding Author: m.feddaoui@uiz.ac.ma*

Abstract—**A numerical study of buoyancy-driven fluid flow and heat transfer on natural convection for water-Al_2O_3 nanofluid filled in square cavity was investigated. The horizontal walls are partially active, the top surface was partially exposed to convection while the bottom wall is partially kept at a constant temperature T_h. The remaining portions of the top and bottom walls are insulated. The governing equations were discretized using the finite volume method and SIMPLER algorithm. A parametric study was undertaken by analyzing the effects of the Rayleigh number, Biot number, length of the exposed portions, and volume fraction of nanoparticles on the fluid flow and heat transfer. It was found from the obtained results that the mean Nusselt number increased with increase in Rayleigh number and volume fraction of nanoparticles regardless the length of the exposed portions of the enclosure.**

Moreover, at high Rayleigh numbers, it was observed that the Al_2O_3-water nanofluid is more effective to enhance the heat transfer rate while at low Rayleigh numbers it does less. Also it was found that the rate of heat transfer increased with increase in nanoparticles volume fraction.

Keywords— **Nanofluid;Enclosure;Heat transfer; Numerical method.**

Nomenclature

Bi	Biot number,$(\mathrm{Bi} = \mathrm{h_0 H/k_{nf}})$
c_p	specific heat at constant pressure $(\mathrm{J\ kg^{-1}K^{-1}})$
g	gravitational acceleration $(\mathrm{m.\,s^{-2}})$
h	local heat transfer coefficient $(\mathrm{W\ m^{-2}K^{-1}})$
H	distance between the bottom and top plates (m)
K	thermal conductivity $(\mathrm{W\ m^{-1}K^{-1}})$
ℓ	length of the exposed portion (m)
L	non-dimensional length of the exposed portion to convection, $\mathrm{L} = \ell/\mathrm{H}$ (see Fig.1)
Nu	Nusselt number, $\mathrm{Nu} = \mathrm{hH/k_f}$
Pr	Prandtl number, $\mathrm{Pr} = \vartheta_\mathrm{f}/\alpha_\mathrm{f}$
q_w	heat flux, $(\mathrm{W\ m^{-2}})$
Ra	Rayleigh number, $\mathrm{Ra} = \mathrm{g\beta(T_H - T_C)H^3/\vartheta_f\alpha_f}$
T	dimensional temperature (°C)
u, v	dimensional x and y components of velocity$(\mathrm{m\ s^{-1}})$
U, V	dimensionless velocities, $\mathrm{U} = \mathrm{uH/\alpha_f}\ \mathrm{V} = \mathrm{vH/\alpha_f}$
W	width of the enclosure (m)
X, Y	dimensional coordinates, $\mathrm{X} = \mathrm{x/H}, \mathrm{Y} = \mathrm{y/H}$
x, y	dimensional coordinates (m)

Creek symbols

α	thermal diffusivity, (m^2s^{-1})
β	thermal expansion coefficient (K^{-1})
μ	dynamic viscosity (Nsm^{-2})
ϑ	kinematic viscosity (m^2s^{-1})
θ	dimensionless temperature, $\theta = (\mathrm{T - T_C})/(\mathrm{T_H - T_C})$
ρ	density (kgm^{-3})

Subscripts

avg	average
C	Cold
f	Base fluid
H	Hot
nf	nanofluid
P	particle
w	wall

I. INTRODUCTION

Convective heat transfer in nanofluids occurs in many engineering applications such as the cooling systems of electronic components, the building and thermal insulation systems, the built-in-storage solar collectors, the nuclear reactor systems, the food storage industry and the power plant [1]. Free convection heat transfer inside nanofluid filled rectangular cavities with different boundary conditions on the side walls has been studied by many researchers [2-4].

As far as forced convection is concerned, the buoyancy-driven fluid flow and heat transfer in enclosures filled with nanofluids have been studied by several investigations. Khanafer et al. [5] conducted a numerical study on buoyancy-driven heat transfer in rectangular cavity filled with nanofluids. Their results showed that rate of heat transfer increased with increase in nanoparticles volume fraction for entire range of Grashof number considered. Oztop et al. [6] using a numerical simulation studied effect of position of a heater in a cavity with cold vertical and horizontal position increased with increase in Rayleigh number and length of the heater. Similar results were found in work of Jou and Tzeng [7] on numerical study of free convection in differentially heated rectangular cavities filled with a nanofluid. Santra et al. [8] studied free

convection of Cu-water nanofluid in a differentially heated square cavity with consideration of Ostwald-de Waele non-Newtonian behaviour of the nanofluid. They found that heat transfer decreased with increase in the nanoparticles volume fraction for a particular Rayleigh number.

In another numerical study, Abu-Nada and Oztop [9]studied effect of inclination angle of a square cavity on unrestricted convection of Cu-water nanofluid inside it. They discovered that the effects of inclination angle on the rate of heat transfer became insignificant at low Rayleigh numbers.

Oztop and Abu-Nada [10], using the finite volume method, did a numerical study on the unrestricted convection heat transfer in rectangular cavities. Their considered comprises a cold vertical wall, an embedded heater counterpart wall, and insulated horizontal walls. They considered the effects of the Rayleigh number, the cavity aspect ratio, the size and the position of the heater on the wall, and the type of nanofluid on the heat transfer within the cavity. Their results indicated an growth in the average Nusselt number with increasing the volume fraction of the nanoparticles for Rayleigh numbers between 10^3 and 10^5. Moreover the results showed that the length of the heater was important parameter affecting the flow and temperature fields. Numerical investigation of periodic free convection fluid flow and heat transfer inside a nanofluid filled square cavity was done by Ghasemi and Aminissadati [11].

In a numerical study, Mahmoodi [12] explored unrestricted convection fluid flow heat transfer of different based nanofluids in a square cavity. The left and right walls of the cavity are maintained at constant temperature T_C while its top and bottom walls are insulated. A thin heater with the temperature of $T_h(T_h > T_c)$is situated inside the cavity which its position and length is varying. The study revealed the Rayleigh numbers the horizontal located heater have higher Nusselt number compared to the vertical located heater while at high Rayleigh numbers the position of the heater does not affect the heat transfer rate.

Recently Mahmoodi and Hashemi [13] examined numerically unrestricted convection of Cu-water nanofluid in C-shaped cavities. They study indicated the mean Nusselt number increased with increase in Rayleigh number and volume fraction Cu nanoparticles regardless aspect ratio of the enclosure. Arefmansh et al. [14] did a numerical simulation to study unrestricted convection of TiO_2-water nanofluid in the annuli of two differentially-heated square ducts. The outer duct is maintained at a constant temperature Tc while the inner duct is kept at a differentially higher constant temperature Th. Their study indicate increased the width of the gap between the ducts and also the Rayleigh number, multiple eddies are developed in the gap between the top walls the square ducts. Mahmoodi and Mazrouei [15] did a numerical simulation to study unrestricted convection of Cu-water nanofluid inside a square cavity having adiabatic square bodies at its centre. They study indicated at $Ra=10^4$ the average Nusselt number is a decreasing function of nanoparticles volume fraction. Moreover at low Rayleigh numbers (10^3 and 10^5) the rate of heat transfer decreases when the size of the adiabatic square body increases while at high Rayleigh numbers (10^5 and 10^6) it increases.

Based on literature reviews, many studies have been did on natural convection of nanofluids filled enclosure where the top surface was partially exposed to convection and bottom surface was partially heated.The enhancement in heat transfer will be examined under a wide range of volume fraction of nanoparticles, wide range of Rayleigh numbers, Biot number and the length of the partially exposed part to convection.

II. Model and Leading Equations

Fig.1presents a schematic diagram of the differentially heated enclosure where the top and bottom walls were exposed partially to forced convection. The left wall was heated and maintained at a constant temperature (T_H) higher than the right cold wall temperature T_C .The top and bottom walls were exposed to forced convection. The length of the exposed part to convection is denoted by ℓ.

At a constant ℓ where it changes $0 \leq \ell \leq W$. For the case of ℓ=0 the top wall and bottom wall was completely insulated and the case of ℓ=W, the top wall is completely exposed to convection and bottom is isotherm. The enclosure is considered square (i.e., W=H).

The nanofluid is presumed to be incompressible, and the nanoparticles are presumed to be in thermal equilibrium with the water. Moreover, there is no slip between the nanoparticles and the base fluid. The thermophysicals attributes of the base fluid and the nanoparticles are presented in **Table 1**.The attributes of the nanofluid are presumed to be constant with the exception of its density which differs according to the Boussinesq approximation [16].

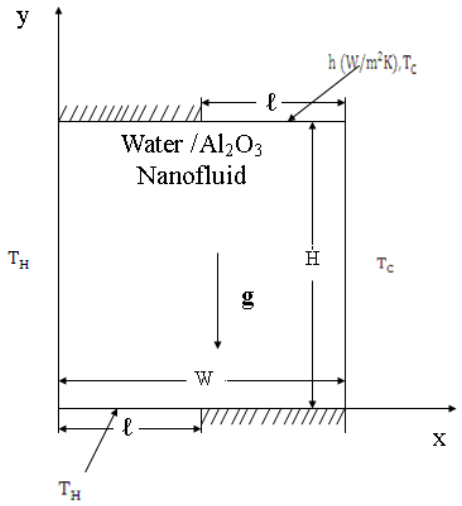

Fig.1 Physical model and coordinate system

Table 1 Thermophysicals properties of the base fluid and nanoparticles [17]

Physical attributes	Base fluid(water)	Nanoparticles(Al_2O_3)
$C_P(J/kg.K)$	4179	765
$\boldsymbol{\rho}(kg/m^3)$	997.1	3970
$\mathbf{k}(W/m.K)$	0.613	25
$\boldsymbol{\beta} \times 10^{-5}(1/K)$	21	0.85

The continuity, x- and y- components of momentum, and energy equations for the two-dimensional fixed and laminar nanofluid flow are given in Eqs.(1)-(4), correspondingly. The natural convection term through the Boussinesq approximation is incorporated into the y component of momentum (Eq. (3)).

$$\frac{\partial u}{\partial x}+\frac{\partial v}{\partial y}=0 \quad (1)$$

$$u\frac{\partial u}{\partial x}+v\frac{\partial u}{\partial y}=\frac{1}{\rho_{nf}}\left[-\frac{\partial p}{\partial x}+\mu_{nf}\left(\frac{\partial^2 u}{\partial x^2}+\frac{\partial^2 u}{\partial y^2}\right)\right] \quad (2)$$

$$u\frac{\partial v}{\partial x}+v\frac{\partial v}{\partial y}=\frac{1}{\rho_{nf}}\left[-\frac{\partial p}{\partial y}+\mu_{nf}\left(\frac{\partial^2 v}{\partial x^2}+\frac{\partial^2 v}{\partial y^2}\right)+(\rho\beta)_{nf}g(T-T_C)\right] \quad (3)$$

$$u\frac{\partial T}{\partial x}+v\frac{\partial T}{\partial y}=\alpha_{nf}\left(\frac{\partial^2 T}{\partial x^2}+\frac{\partial^2 T}{\partial y^2}\right) \quad (4)$$

Where the density, heat capacity, thermal expansion coefficient, and thermal diffusivity of the nanofluid are as follow, respectively [2].

$$\rho_{nf}=(1-\varphi)\rho_f+\varphi\rho_p \quad (5)$$

$$(\rho c_p)_{nf}=(1-\varphi)(\rho c_p)_f+\varphi(\rho c_p)_p \quad (6)$$

$$(\rho\beta)_{nf}=(1-\varphi)(\rho\beta)_f+\varphi(\rho\beta)_p \quad (7)$$

$$\alpha_{nf}=\frac{k_{nf}}{(\rho c_p)_{nf}} \quad (8)$$

To estimation of the dynamic viscosity of the nanofluid the Brinkman model [18] is employed.

$$\mu_{nf}=\frac{\mu_f}{(1-\varphi)^{2.5}} \quad (9)$$

This formula has been used to calculation of the dynamic viscosity of nanofluid in numerical simulation of free convection in recently articles [2-7], [8-10], [12-14].

Using the following dimensionless parameters the governing equation can be converted to dimensionless form.

$$X=\frac{x}{H},\ Y=\frac{y}{H},\ U=\frac{uH}{\alpha_f},\ V=\frac{vH}{\alpha_f},\ P=\frac{pH^2}{\alpha_{nf}{\alpha_f}^2}\ \text{et}\ \theta=\frac{T-T_c}{T_h-T_c} \quad (10)$$

The dimensionless forms of the governing equations are:

$$\frac{\partial U}{\partial X}+\frac{\partial V}{\partial Y}=0 \quad (11)$$

$$U\frac{\partial U}{\partial X}+V\frac{\partial U}{\partial Y}=-\frac{\partial P}{\partial X}+\frac{\mu_{nf}}{\rho_{nf}\alpha_f}\left(\frac{\partial^2 U}{\partial X^2}+\frac{\partial^2 U}{\partial Y^2}\right) \quad (12)$$

$$U\frac{\partial V}{\partial X}+V\frac{\partial V}{\partial Y}=-\frac{\partial P}{\partial Y}+\frac{\mu_{nf}}{\rho_{nf}\alpha_f}\left(\frac{\partial^2 V}{\partial X^2}+\frac{\partial^2 V}{\partial Y^2}\right)+\frac{(\rho\beta)_{nf}}{\rho_{nf}\beta_f}RaPr\theta \quad (13)$$

$$U\frac{\partial T}{\partial Y}+V\frac{\partial T}{\partial Y}=\frac{\alpha_{nf}}{\alpha_f}\left(\frac{\partial^2 T}{\partial X^2}+\frac{\partial^2 T}{\partial Y^2}\right) \quad (14)$$

Where the Rayleigh number Ra, and the Prandtl number Pr are defined as follows:

$$Ra=\frac{g\beta_f H^3(T_h-T_c)}{\vartheta_f\alpha_f},\ \text{and}\ Pr=\frac{\vartheta_f}{\alpha_f} \quad (15)$$

The dimensionless boundary conditions can be written as:
On the left wall; i.e:

$$X=0,\ 0\le Y\le 1\quad U=0,V=0,\qquad \theta=1$$

On the right wall;i.e:

$$X=1,\ 0\le Y\le 1\quad U=0,\qquad V=0,\qquad \theta=0$$

On the bottom wall

$$\begin{cases} Y=0,\quad 0\le X\le L\quad U=0,\ V=0,\ \theta=1 \\ Y=0,\quad L\le X\le 1\quad U=0,V=0,\ \frac{\partial\theta}{\partial Y}=0 \end{cases} \quad (16)$$

On the top wall (exposed length to convection):

$$q''_{conduction}=q''_{convection}-k\frac{dT}{dy}=h(T_w-T_c) \quad (17)$$

Using the non-dimensional quantities given in Eq. (5), from (17), we get

$$\frac{d\theta}{dy}=-Bi\theta_w \quad (18)$$

Where, $Bi=\frac{h_0 H}{k_{nf}}$ is the Biot number defined based on nanofluid attributes, k_{nf} is the thermal conductivity of the nanofluid and h_0 is the local heat transfer coefficient between the fluid surrounding the enclosure and the top wall. Therefore, the boundary conditions on the exposed portion to forced convection at the top wall are:

$$\begin{cases} Y=1,0\le X\le L\quad U=0,\ V=0,\ \frac{\partial\theta}{\partial Y}=0 \\ Y=1,L\le X\le 1\quad U=0,\ V=0,\ \frac{\partial\theta}{\partial Y}=-Bi\theta \end{cases} \quad (19)$$

The local Nusselt number of the heat source is expressed as:

$$Nu_{local}=\frac{hH}{k_f} \quad (20)$$

Where the heat transfer coefficient is:

$$h=\frac{q_w}{T_h-T_c} \quad (21)$$

The thermal conductivity is calculated as following:

$$k_{nf}=-\frac{q_w}{\partial T/\partial X|_{X=0}} \quad (22)$$

By substituting Eqs (22) and (21) in Eq.(20), the Nuesselt number can be written as:

$$Nu=-\left(\frac{k_{nf}}{k_f}\right)\frac{\partial\theta}{\partial X}\Big|_{X=0} \quad (23)$$

The average Nusselt number of the hot wall is obtained by integrating the lacal Nusselt number along the hot wall as follows:

$$Nu_{avg}=\int_0^1 NudY\Big|_{X=0} \quad (24)$$

III. NUMERICAL IMPLEMENTATION

The mass, momentum, and energy governing equations written in terms of the primitive variables are discretizedusing the finite volume approach and the SIMPLER algorithm. In this method [19], a regular two-dimensional finite difference mesh is generated in the computational domain. Consequently, a squareshaped control volume is generated around each nodal point. The governing equations are then integrated over each

control volume. Subsequently, the derivatives of the dependent variables on the faces of the control volume in the resulting equations are replaced by finite difference forms written in terms of the nodal values of the dependent variables. A second-order central difference scheme is used for the diffusion terms while a hybrid scheme, a combination of upwind and central differences schemes, is employed for the convective terms [19].Carrying out the same procedure for all the control volumes yields system of algebraic equations with nodal values of the dependent variables as unknowns. The set of discretized equations are then solved iteratively yielding the velocity, pressure, and temperature at the nodal points. An under-relaxation scheme is used to obtain converged solutions.

A. Grid independence study

In order to determine a proper grid for the numerical simulation, a grid independence study is done for the natural convection heat transfer in the cavity shown in Fig.1. Grid independence check is also done for case of Bi=∞,$\varphi = 0.1$, L=0.5 and Ra=10^6. Seven different grids, namely 21x21; 41x41; 61x61; 81x81; 101x101; 121x121 and 141x141are employed and for each grid size, average Nusselt number of the hot walls is obtained.

Table 2 shows the average Nusselt number of the hot walls for different grids acquired by the current simulation for Ra=10^6. As it can be observed from the table a 101x101uniform grid is adequately fine to ensure a grid independence solution. Based on these results, an101x101uniform grid is employed to perform all of the subsequent numerical calculations. Moreover, in these numerical simulations, the convergence criterion for temperature, pressure, and velocity is:

$$\text{Error} = \frac{\sum_{j=1}^{m}\sum_{i=1}^{n}|\xi^{t+1}-\xi^{t}|}{\sum_{j=1}^{m}\sum_{i=1}^{n}|\xi^{t+1}|} \leq 10^{-7} \qquad (25)$$

Where m and n are the number of meshes in the *x* and *y* direction, correspondingly, ξ is a transport quantity and *t* is number of iteration.

B. Benchmarking of the code

In order to validate the numerical procedure, two simulations of a buoyancy-driven fluid flow and heat transfer in a differentially-heated square cavity filled with air, and a natural convection heat transfer in a partially-heated square cavity filled with the Cu-water nanofluid are executed using the proposed code, and the results are compared with the existing results in a differentially-heated square cavity. The left and right side walls of the cavity are maintained at constant temperatures T_h and T_c, correspondingly, with $T_h > T_c$. The cavity's top and bottom walls are insulted. The cavity is filled with air (Pr=0.72), and the simulations are executed for a range of Rayleigh numbers from 10^3 to 10^6.**Table 3** shows comparisons between the average Nusselt numbers of the hot wall acquired by the present simulation with the results of other investigations [2,14,20-23]for different Rayleigh numbers . As the table shows, very good agreements exist between the results of the current simulation and those of other investigators for the considered range of Rayleigh numbers.

The present numerical solution is further validated by comparing the present code results for Ra=10^5 and Pr=0.70 against the experimental by Krane and Jesse [24] and numerical simulation of Abu-Nada et al. [9]. It is clear that the present code is in good agreement with other work reported in the literature as shown in Fig.2.

Table 2 Grid independence study

Grid size	Nu_{avg}
21×21	9.06301
41×41	8.18205
61×61	7.99956
81×81	7.91824
101×101	7.89731
121×121	7.88586
141×141	7.88475

Table 3 Average Nusselt number for differentially heated square cavity filled with air, comparison with the results of other investigators.

	Ra=10^3	**Ra=10^4**	**Ra=10^5**	**Ra=10^6**
Present study	1.134	2.248	4.546	8.996
Arefmansh et al. [14]	1.113	2.254	4.507	8.802
Khanafer et al. [5]	1.118	2.245	4.522	8.826
Barakos and Mitsoulis[20]	1.114	2.245	4.510	8.806
Fusegi et al. [22]	1.105	2.302	4.646	9.012
Markatos and Pericleous [25]	1.108	2.201	4.430	8.754
Vahl Davis [22]	1.118	2.243	4.519	8.799

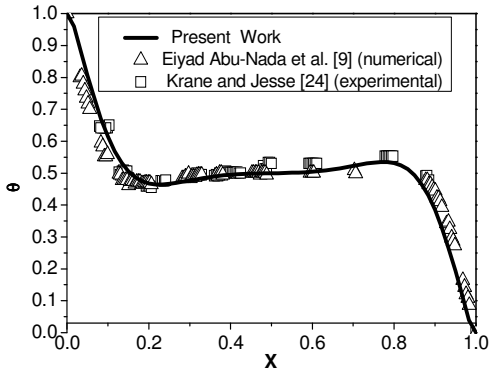

Fig.2 Comparison of results with literature [9, 24].

IV. RESULTS AND DISCUSSIONS

Fig .3 show the streamlines (on the left) and isotherms (on the right) for different Biot numbers at Ra=10^5, l=0.5L and φ=0.1. For Bi=0, demonstrated the typical natural convection problem and bottom wall is heated, the top wall is completely insulated. For Bi=10 illustrates started that the flow strength increase with increasing of Biot number. For Bi=∞, the isotherms at the top partial exposed.

For the case of Bi=∞, Fig.4 portrays effects of partial exposed length (L) on the flow and heat patterns. It is noticed that flow strength is directly related to L. Shape of main cell and its inclination from horizontal is affected by L. Also, is

evident how the thermal boundary layer at the heated wall is affected by L where the thickness of the thermal boundary layer approached zero at the upper end of the left heated wall for the case of L=1.0, which make the heat transfer more effective at the upper portion of the heated wall.

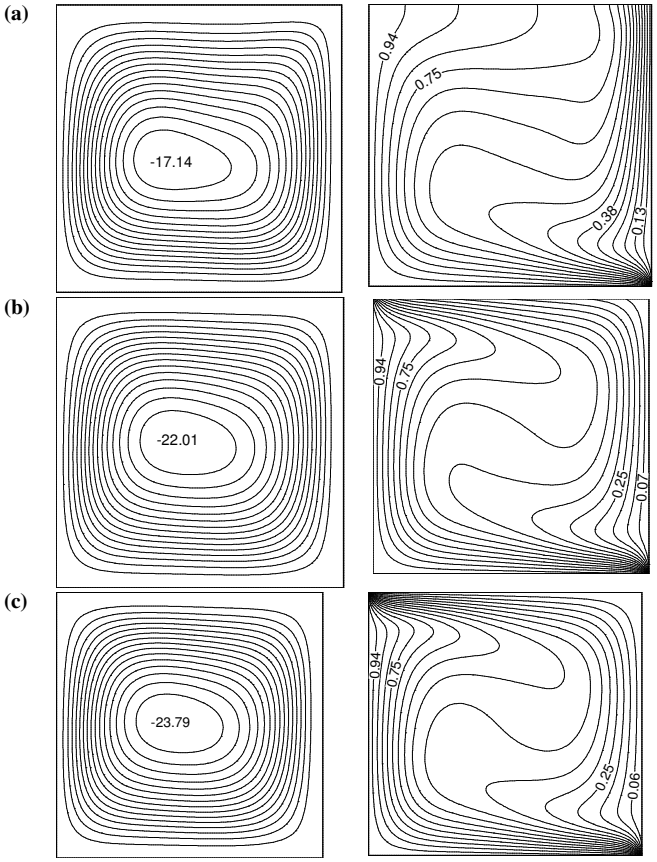

Fig.3 Effects of Biot number on streamlines (left column) and isotherms (right column) for $Ra=10^5$, L=1.0 and φ=0.1 :(a) Bi=0 ;(b) Bi=10 ;(c) Bi=∞

Fig .5 shown the effect of volume fraction of nanoparticles on the streamlines and isotherms for $Ra=10^5$, Bi= ∞ and L=0.5. It is present that more addition of nanoparticles causes the flow strength to increase since the heat transfer within the fluid is enhanced due to the presence of high thermal conductivity of nanoparticles which enhances thermo convection motion within the enclosure and accordingly the flow strength.

Fig. 6 is present to show effect of increase in Rayleigh number on local Nusselt number along the left wall of the enclosure filled with pure fluid for different length of the exposed portion, separately. For L=0.25, the effect of increase in Rayleigh number distribution is more evident along the left wall. As mentioned before, heat transfer along the top wall occurs mainly through conduction; hence increase in Rayleigh number does not affect the rate of heat transfer significantly. Also with increase in Rayleigh number, the point of maximum heat transfer moves to lower region of the hot wall.

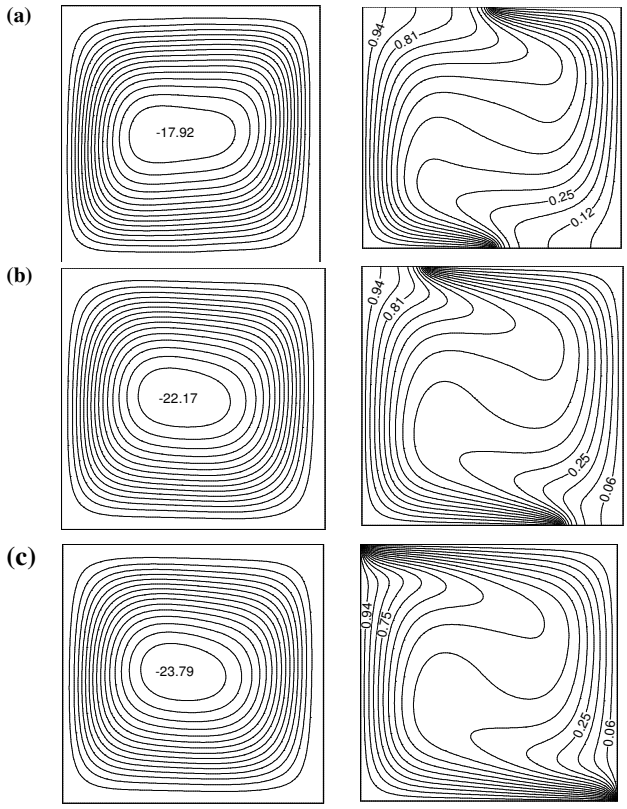

Fig.4 Effects of length on streamlines (left column) and isotherms (right column) for $Ra=10^5$, Bi=∞ and φ=0.1 :(a) L=0.5 ;(b) L=0.75 ;(c) L=1.

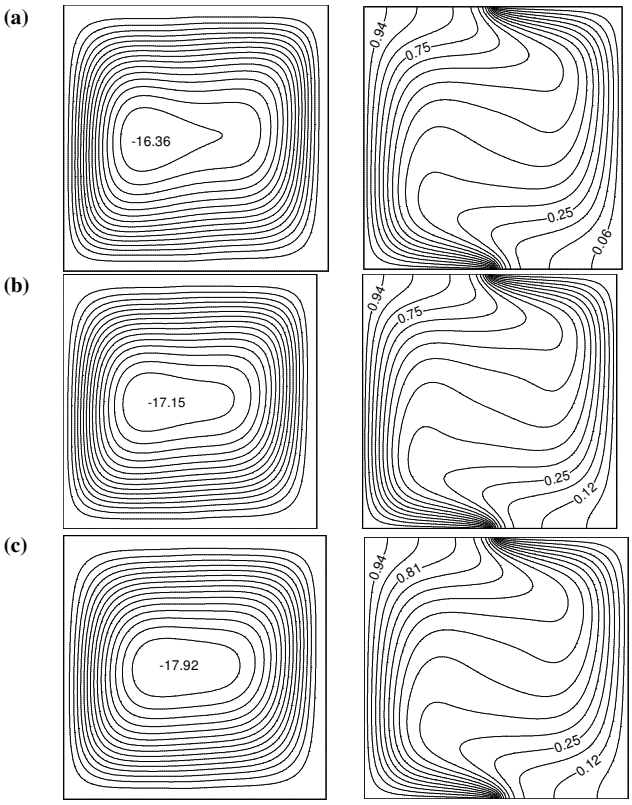

Fig.5 Effects of volume fraction on streamlines (left column) and isotherms (right column) for $Ra=10^5$, Bi=∞ and L=0.5 :(a) φ=0 ;(b) φ=0.05 ;(c) φ=0.1

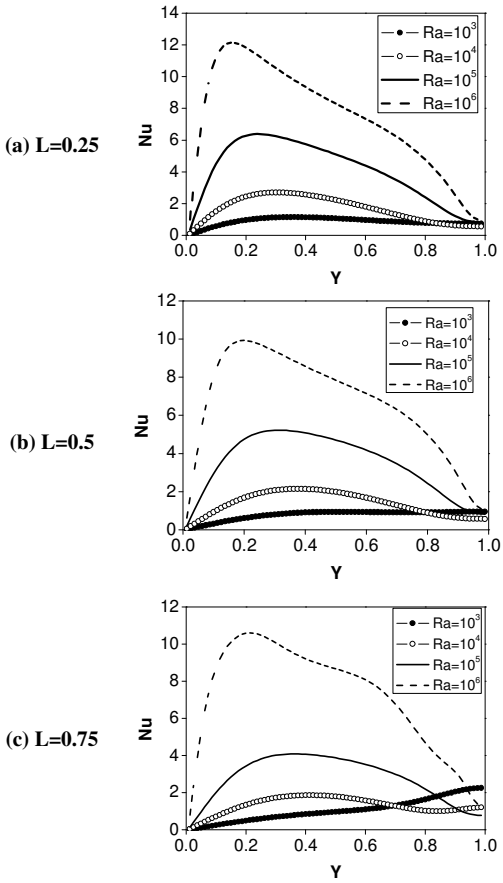

Fig. 6 Variation of local Nusselt number along the left wall of the enclosure filled with pure ($\varphi = 0$) fluid versus Rayleigh numberfor Bi=∞: (a) L=0.25 (b) L=0.5 (c) L=0.75

Effects of increase in the length of the exposed portions on the local Nusselt number along the left wall of the cavity filled with nanofluid at different Rayleigh numbers are illustrated in Fig.7. At Ra=10^3 for all length of the exposed portions, maximum local Nusselt number occurs at the lower end of the hot wall. When the fluid ascends adjacent to the hot wall the fluid temperature decreases, then the temperature gradient increases; hence the local Nusselt number increases. For L=0.25 minimum local Nusselt number occurs at the upper part of the hot wall. Also for this size of the exposed portions, a uniform Nusselt number distribution is observed along whole upper half of the hot wall. At Ra=10^3 the local Nusselt number increases when length of the exposed portions decreases.

For L=0.5 and 0.75 the local Nusselt increases from down to the middle section of the hot wall and then increases by moving towards the top of the wall. At Ra=10^4 and 10^5, maximum rate of heat transfer occurs at lower end of the hot wall. Maximum local Nusselt number at the lower end of the hot wall occurs for the cavity with L=0.25. With decrease in L, the maximum local Nusselt number increases for $Y \leq 0.3$. A reverse behavior is found for the major portion of the wall. For $Y \geq 0.3$ the local Nusselt number decreases when L decreases. It is because of increase in blockage of fluid flow via increase in the length of the exposed portions.

At Ra=10^6 the length of the exposed portions does not affect the Nusselt number distribution significantly. At high Rayleigh numbers, boundary layers are formed adjacent to the isothermal side walls and fluid existing in core of the cavity in nearly stagnant.

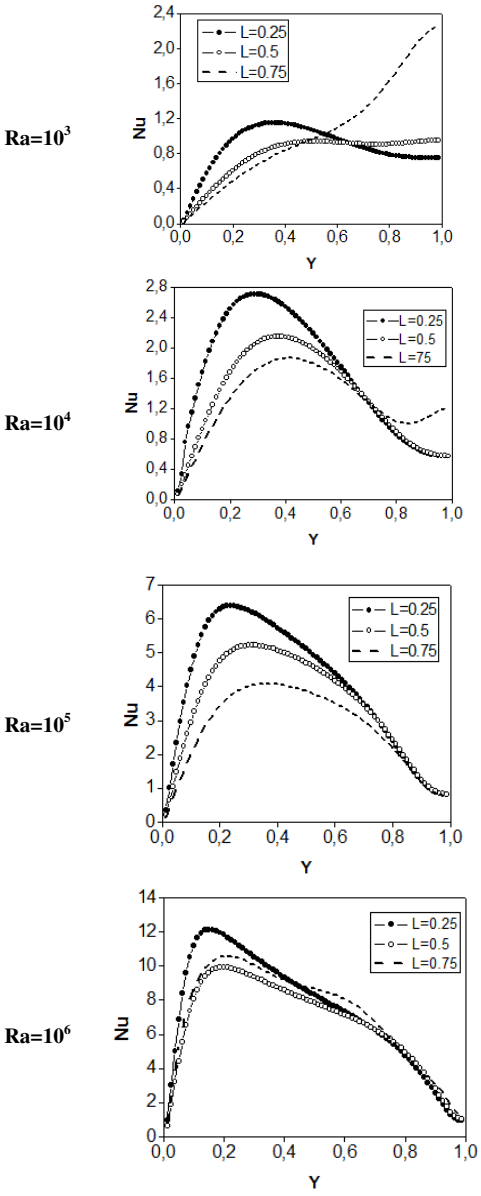

Fig. 7 Variation of the local Nusselt number with length of the exposed portion at different Rayleigh numbers for φ=0.1 and Bi=∞.

Effects of nanoparticles volume fraction on local Nusselt number along the left wall of the enclosures with L=0.5 at different Rayleigh numbers are illustrated in Fig.8. As can be seen from the figure at Ra=10^3 the local heat transfer increase in nanoparticles volume fraction for all range of Rayleigh number considered and along all portions of the wall.

At this Rayleigh number for the cavity with an exposed to partial convection with L=0.5 the increase in the nanoparticles volumes fraction does not affect local Nusselt number distribution significantly.

At Ra=10^4, 10^5 and 10^6 the local Nusselt number at the lower end of the hot wall increases when the nanoparticles volume fraction increases while with moving upward along the wall, the effect of the nanoparticles concentration on increase of the rate of heat transfer decreases and finally a similar local Nusselt number for the nanofuid and pure fluid occurs in the upper end of the hot wall.

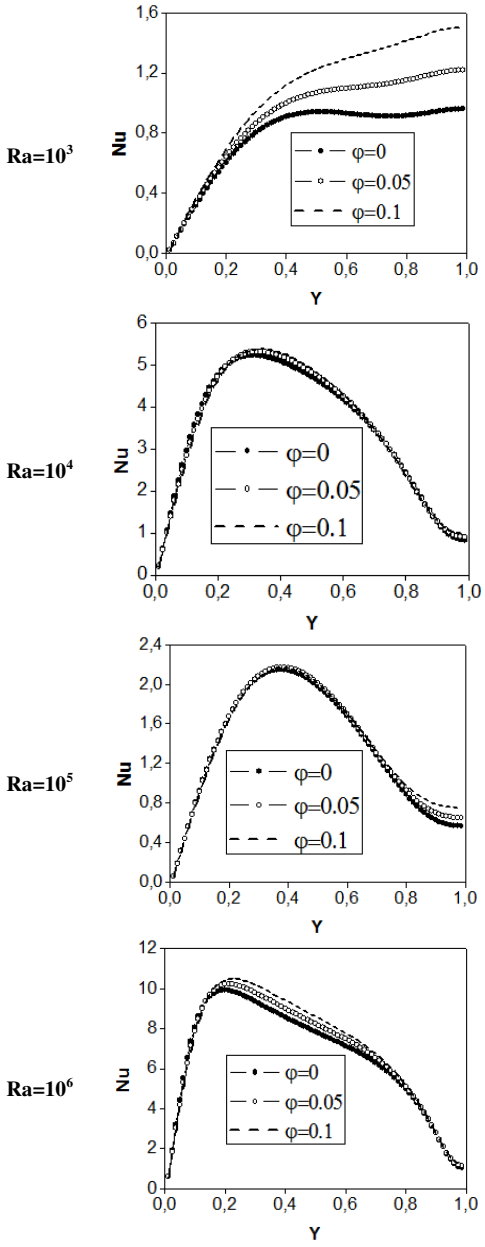

Fig.8 Variation of the local Nusselt number with the volume fraction of the nanoparticles at different Rayleigh numbers for L=0.5 and Bi=∞.

Fig.9 shows the effect of the Biot number Bi on the local Nusselt number at different Rayleigh numbers distribution at the heated wall. At Ra=10^3 the local Nusselt increases when Biot number increases.

For Bi=10 and ∞ the local Nusselt increases from down to the middle section of the hot wall and then increases by moving towards the top of the wall.

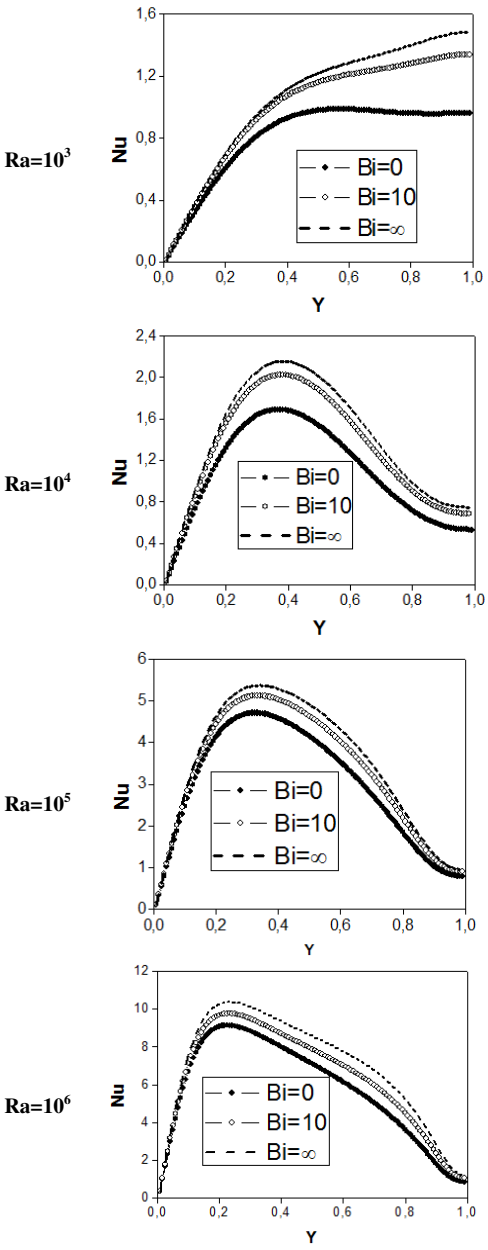

Fig.9. Variation of the local Nusselt number with the Biot number at different Rayleigh numbers for L=0.5 and φ=0.1.

At Ra=10^4 and 10^5, maximum rate of heat transfer occurs at lower end of the hot wall. Maximum local Nusselt number at the lower end of the hot wall occurs for the cavity with L=0.25. With increase in Bi, the maximum local Nusselt number increases for $Y \leq 0.3$. A reverse behavior is found for the major portion of the wall. For $Y \geq 0.3$ the local Nusselt number decreases when values Bi decreases. It is because of increase in blockage of fluid flow via higher values of Bi.

At Ra=10^6 the Biot number does not affect the Nusselt number distribution significantly. With higher values of Bi, the maximum local Nusselt number increases for ≤ 0.2 . A reverse behavior is found for the major portion of the wall.

For $Y \geq 0.2$ the local Nusselt number decreases when Bi decreases.

At this Rayleigh number for the cavity with an exposed to partial convection with L=0.5 the increase in the nanoparticles volumes fraction does not affect local Nusselt number distribution significantly.

At Ra=10^4, 10^5 and 10^6 the local Nusselt number at the lower end of the hot wall increases when the nanoparticles volume fraction increases while with moving upward along the wall, the effect of the nanoparticles concentration on increase of the rate of heat transfer decreases and finally a similar local Nusselt number for the nanofluid and pure fluid occurs in the upper end of the hot wall.

V. CONCLUSION

In the present paper the thermal and flow field due to buoyancy force in a square enclosure where the top surface was partially exposed to convection and bottom is isotherms filled with water based Al_2O_3-water nanofluid was investigated numerically using the finite volume method and SIMPLER algorithm.

A parametric study involving the effects of the Biot number, non-dimensional length of the exposed portions (L), and the Al_2O_3 volume fraction on the annuli fluid flow and heat transfer are conducted. The observed results showed that for the case of high Biot number the heat transfer along the heated is enhanced by increasing the Rayleigh number. However, the enhancements are less pronounced at the top portion of the heated wall$(y > 0.9)$. When the top wall is totally exposed to convection and bottom wall is isotherm, the results prevail that heat transfer is more efficient at high Biot number especially at the top portion of the heated wall. For the case of high Biot number, the results show that the heat transfer at the upper portion of the heated wall increase considerably at high L and for $L \leq 0.75$ the effect of L is less pronounced. For all considered cases, when the volume fraction of the nanoparticles is kept constant, the rate of heat transfer increases of the Rayleigh number.

At Ra=10^3, 10^4, and 10^5, when the volume fraction of the nanoparticles is kept constant, the rate of heat transfer increase with decreasing length of the exposed portions.

At Ra=10^3, 10^4, and 10^5, when the Rayleigh number is kept constant, the average Nusselt number increases by increase in volume fraction of the nanoparticles.

Effect of nanoparticles on enhancement of heat transfer at low Rayleigh number is more significant than that at high Rayleigh numbers.

REFERENCES

[1] S. Ostrach, Natural convection in enclosures, Journal of Heat Transfer, vol. 10, pp. 1175-1190, 1988.

[2] M.A.R. Sharif, T.R. Mohammad, Natural convection in cavities with constant flux heating at the bottom wall and isothermal cooling from the sidewalls, International Journal of Thermal Science, vol.44, pp. 865-878, 2005.

[3] B. Calcagni, F. Marsili, M. Paroncini, Natural convective heat transfer in square enclosures heated from below, Applied Thermal Engineering, vol.25, pp. 2522-2531, 2005.

[4] A. K. Sharma, K. Velusamy, C. Balaji, Turbulent natural convection in an enclosure with localized heating from below, International Journal of Thermal Science , vol. 46, pp. 1232-1241, 2007.

[5] K. Khanafer, K. Vafai, M. Lightstone, Buoyancy-driven heat transfer enhancement in a two-dimensional enclosure utilizing nanofluid, Int. J. Heat Mass Transf. vol. 46, pp. 3639-3653, 2003.

[6] H.F. Oztop, I. Dagtekin, A. Bahloul, Comparison of position of a heated thin plate located in cavity for natural convection, Int. Commun. Heat Mass Transfer, vol. 32, pp. 94-106, 2005.

[7] R.Y. Jou, S.C. Tzeng, Numerical research of nature convective heat transfer enhancement filled with nanofluids in rectangular enclosures, International Communication in Heat and Mass Transfer, vol. 33, pp. 727-736, 2006.

[8] A.K. Santra, S. Sen, N. Chakraborty, Study of heat transfer augmentation in a differentially heated square cavity using copper-water nanofluid, International Journal of Thermal Science, vol. 47, pp. 1113-1122, 2008.

[9] E. Abu-Nada, H.F. Oztop, Effect of inclination angle on natural convection in enclosure filled with Cu-Water nanofluid, Int.J.Heat Fluid Flow, vol. 30, pp. 669-678, 2009.

[10] H.F. Oztop, E. Abu-Nada, Numerical study of natural convection in partially heated rectangular enclosures filled with nanofluids, Int. J. Heat Fluid Flow, vol. 29, pp. 1326-1336, 2008.

[11] B. Ghasemi, S.M. Aminossadati, Periodic natural convection in a nanofluid filled enclosure with oscillating heat flux, International Journal of Thermal Science, vol. 49pp. 1-9, 2010.

[12] MostafaMahmoodi, Numerical simulation of unrestricted convection of nanofluide in a square cavity with an inside heater, International Journal of thermal Sciences, vol. 50, pp.2161-2175, 2011.

[13] MostafaMahmoodi, Seyed Mohammad Hashemi, Numerical study of natural convection of a nanofluid in C-shaped enclosures, International Journal Sciences, vol. 55, pp. 76-89, 2012.

[14] A. Arefmanesh, M.Amini, M.Mahmoodi, M.Najafi, Buoyancy-driven heat transfer analysis in two-square duct annuli filled with a nanofluid, European Journal of Mechanics B/Fluids, vol. 33, pp. 95-104, 2012.

[15] M.Mahmoodi, S.M. Sebdani, Natural Convection in a Square Cavity Containing a Nanofluid and an Adiabatic Square Block at the Centre, Superlattices and Microstructures, vol. 52, pp. 261–275, 2012.

[16] A. Bejan, Convection Heat Transfer, John Wiley & Sons, Inc., Hoboken, New Jersey, USA, 2004.

[17] Hakan F.Oztop, Eiyad Abu-Nada, Yasin Varol, Khaled Al-Salem, Computational analysis of non-isothermal temperature distribution on natural convection in nanofluid filled enclosures, Suerlattices and Microstructures, vol. 49, 453-467, 2011.

[18] H.C Brinkman, The viscosity of concentrated suspensions and solutions, Journal of chemical Physics, vol. 20, pp. 571-581, 1952.

[19] S.V. Patankar, Numerical Heat Transfer and Fluid Flow, Hemisphere Publishing Corporation, Taylor and Francis Group, New York, 1980.

[20] G. Barakos, E. Mitsoulis, Natural convection flow in a square cavity revisited: laminar and turbulent models with wall fraction, Int.J. Numer.Meth.Fluid., vol. 18, pp. 695-719, 1994.

[21] G.V. Davis, Natural convection of air in a square cavity, a benchmark numerical solution, Int. J. Numer. Meth.Fluid. vol. 3, pp. 249-264, 1983.

[22] T. Fusegi, J.M. Hyun, K. Kawahara, B. Farouk, A Numerical study of tree-dimensional natural convection in a differentially heated cubical enclosure, Int. Heat Mass Transfer. vol.34, pp. 1543-1557, 1991.

[23] N.C. Markatos, K.A. Pericleous, Laminar and turbulent natural convection an enclosed cavity, Int.J.Heat Mass Transf. vol. 27, pp. 772-775, 1984.

[24] R.J. Krane, J. Jessee. Some detailed field measurements for a natural convection flow in a vertical square enclosure, in: 1st ASME-JSME Thermal Engineering Joint Conference 1 (1983) 323-329.